A mathematical mould model for transient infiltration and lubrication behaviour of slag in a steel continuous casting process

by M-H. Cao[1], B. Yu[1], C. Zhou[2], and X-Z. Zhang[1]

Affiliation:
[1]National Engineering Research Centre for Equipment and Technology of Cold Rolled Strip, Yanshan University, Qinhuangdao, China.
[2]Ocean College, Hebei Agricultural University, Hebei, China.

Correspondence to:
X-Z. Zhang

Email:
zhangxzh@ysu.edu.cn

Dates:
Received: 12 Oct. 2023
Revised: 16 Feb. 2024
Accepted: 29 Feb. 2024
Published: March 2024

How to cite:
Cao, M-H., Yu, B., Zhou, C., and Zhang, X-Z. 2024
A mathematical mould model for transient infiltration and lubrication behaviour of slag in a steel continuous casting process.
Journal of the Southern African Institute of Mining and Metallurgy, vol. 124, no. 3. pp. 147-152

DOI ID:
http://dx.doi.org/10.17159/2411-9717/3158/2024

Synopsis

The transient infiltration and lubrication behaviour of slag during continuous casting of steel is important for billet quality. A two-dimensional coupled mathematical mould model was developed to investigate these phenomena. The accuracy of the model was verified by comparing the calculated slag consumption with measurements by the plant. The results show that the liquid slag is consumed from the middle and late period of positive strip time to the next early period of positive strip time, including the entire negative strip time. The maximum downward infiltration velocity and positive pressure in the slag channel is at the middle of the negative strip time. Increasing the positive pressure of the slag channel is conducive to lubrication. The shear stresses acting on the shell surface and at the mould side were determined by the lubrication slag consumption and total slag consumption, respectively, and gradually decreased with increasing slag consumption. The negative strip time was lengthened to increase the slag consumption and prolong the time near the maximum downward shear stress, so as to be conducive to the demould.

Keywords

lubrication, slag consumption, slag infiltration, shear stress, continuous casting.

Introduction

Most of the world's steel is produced by the continuous casting process, in which molten steel is continuously injected into a water-cooled mould. The molten steel solidifies along the mould wall, and the semi-finished billet is continuously pulled from the lower part of the mould (Youming, Yeming, and Kuangdi, 2022). Billets with diverse sizes, shapes, and qualities are produced. Continuous casting has the advantages of high quality products and cost efficiency (Louhenkilpi, 2014).

The slag plays an important role in continuous casting by providing effective heat insulation (Yang *et al.*, 2020) and lubrication (Zhang *et al.*, 2018; Yan *et al.*, 2019), preventing secondary oxidation of molten steel and improving heat transfer within the mould. Liquid slag infiltrates from the slag pool into the gap between the shell and mould wall, forming a slag film that is conducive to lubrication and prevents the shell from sticking to the mould wall.

The behaviour of slag in the continuous casting process has been the subject of numerous studies. A semi-empirical model was proposed by Shin *et.al.* (2006) to predict slag consumption based on plant measurements, but a description of transient slag consumption was omitted. The phenomenon of slag infiltration and initial shell solidification in the meniscus was characterized though an integrated model (Ramirez-Lopez *et al.*, 2010; Ramirez-Lopez, Lee, and Mills, 2010). The total slag consumption near the meniscus was calculated, but the result was slightly higher than that shown from plant data. Jonayat and Thomas (2014) studied the effects of casting parameters on slag consumption by a computational model of the meniscus region; however, the meniscus shape was prefixed and the solidified shell was not considered. Yang, Meng and Zhu (2014, 2018) described the transient pressure variation of liquid slag in the channel using a cold model, and analysed the impact of casting speed on liquid slag consumption by means of a two-dimensional coupling model. The impact of the modification ratio (α) of non-sinusoidal oscillation on slag lubrication was investigated by Yan *et al.*, (2019) but the model only took into account the liquid slag consumption. Zhang *et al.* (2019a, 2019b, 2021) investigated the infiltration of slag, and compared the effects of different casting parameters on total slag consumption. Slag infiltration at the corner of the mould was described by Ji *et al.* (2023) through a three-dimensional mathematical model. However, there was little information considered regarding the evolution of lubrication consumption of liquid slag and friction. Understanding the infiltration and lubrication behaviour of slag was found conducive to smoothly demolding of the shell from the mould and improving lubrication between the slab and the mould.

In the current work we established a coupled model to investigate the transient infiltration and lubrication behaviour of slag. The accuracy of the model was verified by comparing the calculated slag consumption with measurements by the plant. The transient variation in infiltration velocity of slag in the slag channel, pressure in the slag channel, thickness of the liquid and solid slag layers, shell surface temperature, heat flux of the copper plate, total slag consumption, lubrication consumption, the shear stress of the liquid slag on the shell surface, and shear stress at the mould wall were monitored at 300 mm below the meniscus. The transient infiltration of slag and slag lubrication were analysed, providing a theoretical basis for controlling the slag consumption and shear stress, thereby enhancing the lubrication effect of the slag and improving the surface quality of billets.

Description

Assumptions

The assumptions were proposed based on describing the industrial production of continuous cast slab through numerical simulation calculation:

- Due to the symmetry of the flow and temperature fields in the mould, half of the mould was used as the calculation domain.
- Molten steel is an incompressible Newtonian fluid.
- The impact of mould taper on flow and heat transfer were not taken into consideration, and the dimensional change of casting slabs caused by solidification cooling shrinkage was ignored.
- The solid-liquid phase was considered a porous medium during solidification.

Model description

The mould model included the submerged entry nozzle (SEN), copper plate, and fluid domain (steel-slag-air), as shown in Figure 1a. The steel surface was covered with slag and air, each with a thickness of 50 mm. ICEM was used to build the mesh. The total amount of mesh elements was 168 962, and the area near the fluid-solid interface was subjected to mesh refinement with a minimum mesh size of 50 μm (Figure 1b).

Fluid flow, heat transfer, and solidification during the continuous casting process were included in the model. ANSYS Fluent 19.2 was employed to solve the Navier-Stokes equations. The volume of fluid method (VOF) was used to calculate the phase fractions. The interface was tracked by continuous surface forces (CFS). The k-ε model was utilized to solve turbulent flow. The solidification of fluid was solved by using the solidification model.

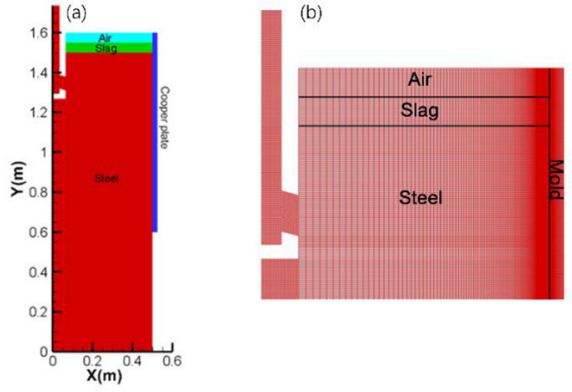

Figure 1—(a) Schemes of model , (b) mesh

The boundary settings are shown in Figure 2. The boundary of the upper surface was set as a free surface with a temperature of 300 K. The boundary of the mould outlet was set to outflow, resulting in a fully developed flow at this boundary. The interface between the fluid and solid was defined as a coupled wall, the fluid-mould interface was coupled in terms of velocity and heat flux, and oscillated with the mould. The walls of the SEN and top and bottom walls of the mould were set as insulated due to the negligible heat flux across these walls in the real process. A symmetric boundary condition was applied for the plane of symmetry. The boundary of the SEN inlet was set to velocity inlet, where the inlet velocity (V_{in}) was determined by the mass balance as shown in Equation [1], and the inlet temperature was 1830 K. The cold wall of the copper plate was set as a convection boundary with the water temperature 305 K and the heat transfer coefficient (h_c) as per the empirical determination by Xiang. Xia, and Wu (2023) of 28 000 W/m²K, correlating to a water flow rate of 10 m/s. Similarly, the wall of the secondary cooling zone was set as a convection boundary with the water spray temperature 300 K and heat transfer coefficient (h_s) 2000 W/m²K correlating to a specific water flow in the secondary cooling zone of 1.03 L/kg as determined by Zang *et al.* (2019). The oscillation mode of the mould was sinusoidal. The velocity and displacement expressions of mould oscillation are illustrated in Equations [1]–[3]. A dynamic mesh was employed to achieve the oscillation of the mould.

$$V_{in} = \frac{A_{out} \times V_c}{A_{in}} \quad [1]$$

where V_c is the casting speed (m/min), A_{in} the inlet area (m²), and A_{out} the outlet area (m²).

$$V_m = \frac{4Mhf\pi \cos\{2\arctan[Mtan(\pi ft)]\}}{1+M^2+(1-M^2)\cos(2\pi ft)} \quad [2]$$

$$M = \cot\left[\frac{\pi}{4}(1+\alpha)\right]$$

$$S_m = hsin\{2\arctan[Mtan\pi ft]\} \quad [3]$$

where V_m is the mould velocity (m/s), h the oscillation amplitude of the mould (m), f the oscillation frequency (Hz), α the modification ratio (sinusoidal mode when α was zero), and S_m mould displacement (m).

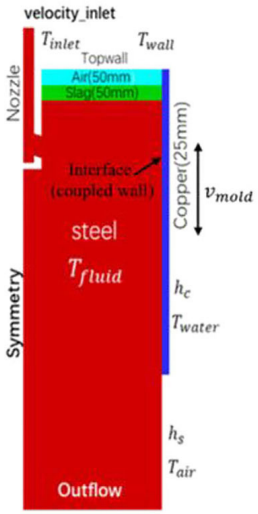

Figure 2—Boundary of the model

The break temperature of the slag was utilized to distinguish the liquid and solid phases since the formation of the first solids in the liquid slag is related to the break temperature (Kölbl, and Harmuth, 2019). The time step of the solution was 0.0001 seconds, and the results were calculated for more than a month of casting. The detailed governing equation, casting parameters, model parameters, and material properties are described elsewhere (Cao *et al.*, 2023).

Validation of slag consumption

The model was validated in Cao *et al.* (2023) by comparing the oscillation marks with plant measurements and the pitch of oscillation marks with the theoretical values, respectively. In addition, the 17 cases in Table I were simulated, and the slag consumption was calculated during one cycle after the calculation was stable. The slag consumptions were compared with the plant measurements (Shin *et al.*, 2006). Figure 3a shows that the calculated slag consumption was in good agreement with the plant measurements. The slag consumption decreased with increasing casting speed (Figure 3b), which is consistent with observations by Shin *et al.* (2006)

Based on the above, the depth of the oscillation mark and the slag consumption were compared with the plant measurements. The two-dimensional model showed good accuracy and robustness, and hence could be used to study the lubrication behaviour of slag.

Results and discussion

Under the mould oscillation for f = 174 cpm, h = 2.9 mm, α = 0 with V_c=1.4 m/min, the specific variables at 300 mm below the meniscus were tracked to investigate the transient infiltration of slag and slag lubrication. The velocity and displacement of mould oscillation are presented in Figure 4, where the time period when the downward oscillation velocity exceeds the pulling speed is negative strip time (t_n), and the rest period the positive strip time (t_p).

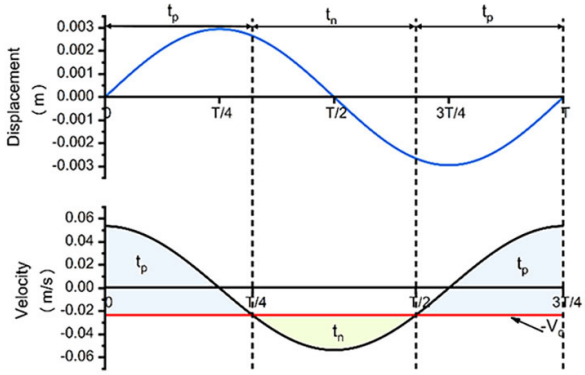

Figure 4—Oscillation velocity and displacement

Table I

Operating conditions and calculated slag consumption

No.	Oscillation amplitude (mm)	Oscillation frequenc, (cpm)	Casting speed (m/min)	Modification ratio	Positive strip time (s)	Slag consumption (g · m/cycle)
1	6	120	0.8	0.1	0.3015	3.148
2	4	120	1.2	0.2	0.3502	3.062
3	4	120	0.8	0.2	0.3347	2.792
4	5	120	0.8	0.2	0.3282	2.488
5	5	120	1.4	0	0.3105	2.462
6	2.9	174	1.4	0	0.2217	1.596
7	5	120	1.2	0.2	0.341	2.476
8	5	120	1.4	0.2	0.3472	2.305
9	6	120	0.8	0.3	0.3453	2.619
10	6	120	1.4	0	0.3001	2.506
11	6	120	1.4	0.2	0.3399	2.095
12	4	120	1.4	0	0.3268	2.83
13	7	120	1.4	0	0.2927	2.648
14	2	174	1.4	0	0.2487	1.852
15	4	120	1.4	0.2	0.3577	2.307
16	6	120	0.8	0.2	0.3238	2.356
17	6	120	1.4	0.1	0.3206	1.967

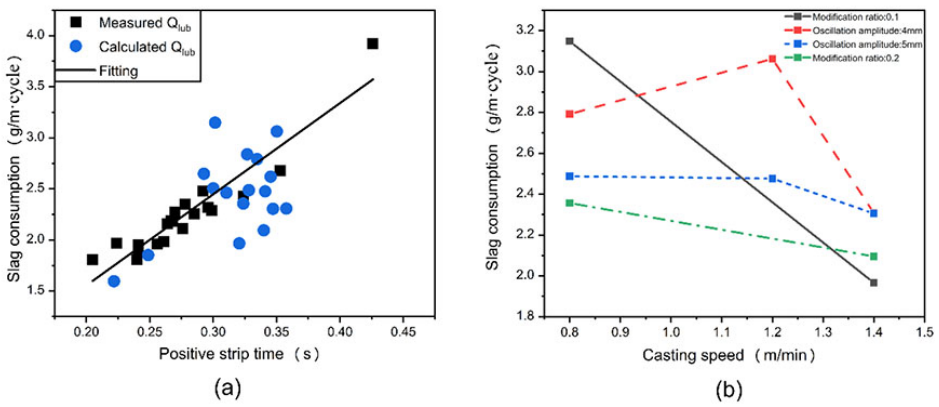

Figure 3—(a) Validation of predicted slag consumption per oscillation cycle with measurements taken at different positive strip times, (b) effect of casting speed on slag consumption in each oscillation cycle

Infiltration velocity of slag and pressure in slag channel

The transient downward infiltration velocity of slag in the slag channel is shown in Figure 5. During the early and late stages of t_p, the slag flowed upward owing to the upward oscillation of the mould. During the t_n, the downward infiltration of the slag was accelerated due to the increase in the downward oscillation velocity of the mould, reaching a maximum of 0.032 m/s at the middle stage, followed by a gradual decrease in infiltration velocity. The infiltration velocity of slag was determined by the velocity and position of mould oscillation.

The variation of the pressure in the slag channel in a cycle is illustrated in Figure 6. The pressure varied between the maximum positive and negative pressures. The slag channel experienced negative pressure during the early and late stages of t_p, with a maximum value of 12 167.55 Pa. However, the slag channel experienced positive pressure during the t_n, reaching a maximum value of 24 671.961 Pa at the middle of the t_n. The pressure in the slag passage was affected by mould oscillation and the movement of the slag rim (Cao *et al.*, 2023).

The variation of slag pressure exerted an influence on the meniscus and the initial shell, resulting in periodic deformations (*i.e.* oscillation marks). Increasing the negative pressure of the slag channel was conducive to enhancing the effect of liquid slag infiltration in the slag channel, and improving the lubrication effect. Increasing the positive pressure of the slag channel was conducive to forced demoulding and preventing breakout. However, an increase in both maximum positive and negative pressures resulted in an increasing pressure difference within the slag channel, exacerbating meniscus fluctuations and initial shell deformations, which is not conducive to improving the surface quality of slabs. Therefore, it was crucial to control these parameters.

Thickness of slag film

The surface temperature of the shell and heat flux of the copper plate are shown in Figure 7. The heat flux was within 1.83 to 3.44 MW/m^2, and the surface temperature of the shell was within the range1487.20 to 1524.13 K. The maximum temperature and minimum heat flux appeared near the t_n. The higher the surface temperature of the shell, the faster the slag melting rate, resulting in a thicker liquid slag layer, which is conducive to lubrication. The greater the heat flux, the thicker the solid slag layer, which is not conducive to the solidification of liquid steel into a shell.

The transient variation in thickness of solid and liquid slag layers is exhibited in Figure 8. The thickness variation of the solid slag layer was inversely related to that of the liquid slag layer, and the thicknesses were 1.31 to 1.37 mm and 0.19 to 0.28 mm, respectively. At the middle of the t_n, the the liquid layer affected by fast flowing slag became thinner and the solid layer became thicker. The maintenance of a thick and uniform liquid slag film, while ensuring a thin solid slag film, was crucial in order to prevent breakout.

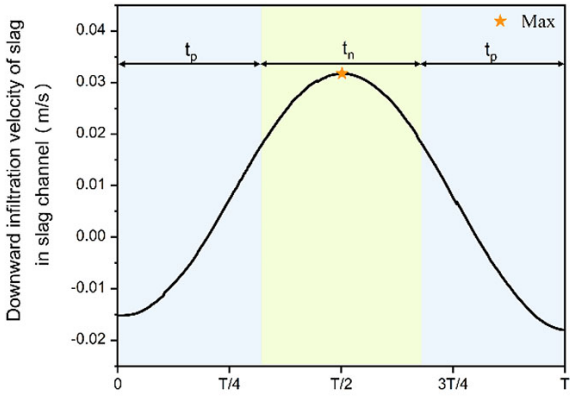

Figure 5—Infiltration velocity of slag in slag channel

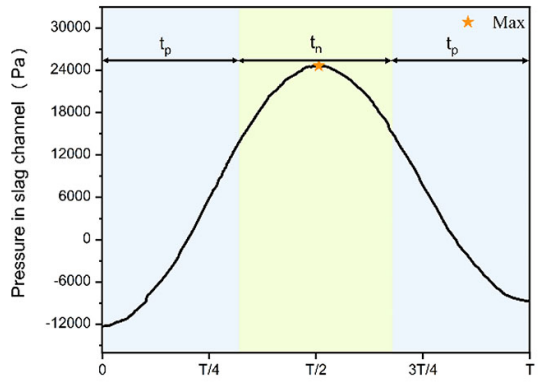

Figure 6—Variation of pressure in channel

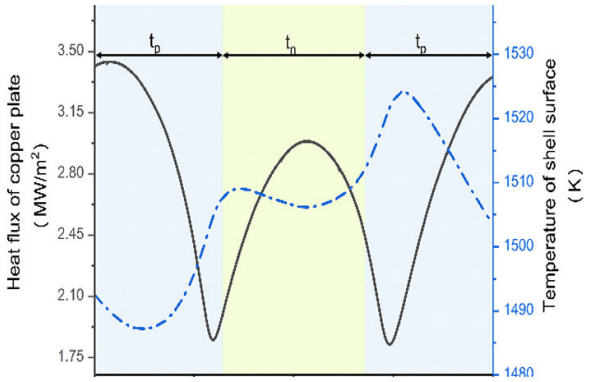

Figure 7—Surface temperature of the shell and heat flux of the copper plate

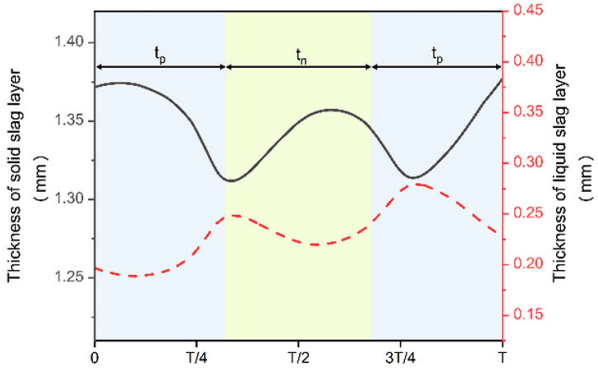

Figure 8—Transient variation in thickness of solid and liquid slag layers

Slag consumption

The slag film could prevent the shell sticking to the mould wall, which contained the liquid and solid layers. The liquid slag layer could help the shell to demould smoothly. The slag consumption was an important index for evaluating the lubrication performance of the slag. The slag consumed in the total slag film was considered as total slag consumption (Q_t, kg/s), while the slag consumed in the liquid slag film was considered as lubrication consumption

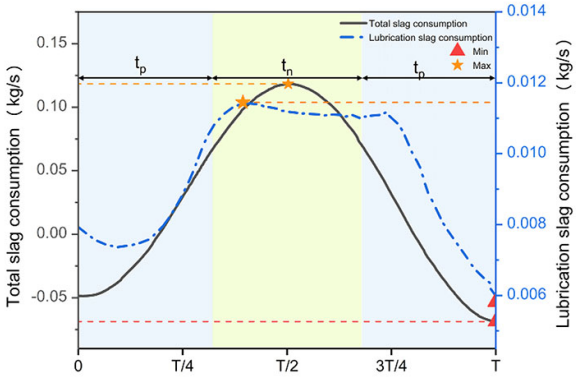

Figure 9—Total slag consumption, lubrication slag consumption, and average slag consumption during the t_n and t_p

(Q_{lub}, kg/s). Transient lubrication consumption and total slag consumption are presented in Figure 9, where the minus sign indicates upward movement of slag.

The slag consumption tended to increase during the t_n.The variation of Q_t and Q_{lub} was similar, with average values of 0.03 and 0.009 kg/s, respectively. The liquid slag was pumped into the slag channel under positive pressure. The maximum Q_t and Q_{lub} were observed near the middle of t_n, with values of 0.118 and 0.011 kg/s, respectively.

The mechanism of liquid slag consumption was elucidated according to the above slag consumption, the flow and pressure of slag in the slag channel, and the variation of slag film thickness. The liquid slag flowed upward due to the upward movement of the mould during the early stage of t_p; the inertial effect weakened and the lubrication consumption increased with the decrease in upward oscillation velocity of the mould. As the upward velocity of the mould decreased to zero and the mould began to oscillate downward, the downward flow of liquid slag was facilitated by the inertial effect of the mould and liquid slag continued to be consumed, reaching the maximum value of 0.0115 kg/s at the initial stage of t_n. After that, although the liquid slag infiltrated into the slag channel under the action of the increased positive pressure and slag infiltration velocity, the decrease in thickness of the liquid slag film led to a decrease in lubrication consumption. The lubrication consumption decreased to 0.0111 kg/s at the middle of t_n. Later, the lubrication consumption began to increase with the increase in thickness of the liquid slag film. With the upward oscillation of the mould, the slag consumption decreased due to the weakening of the suction and the inertial effect of the mould. The lubrication consumption was minimum at –0.0061 kg/s at the end of t_p. Liquid slag was consumed from the middle and late period of t_p to the next early period of t_p, including the entire t_n.

Shear stress

Shear stress acting on the shell surface ($\tau_{s/l}$) and at the mould side ($\tau_{s/l}$), Pa) were important parameters which characterized the slag lubrication and the interaction between the mould wall and shell, and the surface quality of the shell and productivity of continuous casting were directly affected. Hence, $\tau_{s/l}$ and τ_{mold} were calculated according to Equations [4] and [5] (Meng and Thomas, 2003), respectively:

$$\tau_{s/l} = \mu_{slag}\frac{\partial v_y}{\partial x} \quad [4]$$

$$\tau_{mold} = -\int_{x=0}^{d_s}\frac{d\sigma_y}{dy}\cdot dx + \tau_{s/l} = \frac{\nu}{1-\nu}\rho_{steel}gd_s + \tau_{s/l} \quad [5]$$

where: μ_{slag} is the viscosity of the slag(Pa·s), V_y is the vertical velocity of the slag (m/s), ∂_x the thickness of the liquid slag layer (m), σ_y the axial stress in the solid slag layer, d_s the thickness of the solid slag layer (mm), and ν the Poisson's ratio of the slag (0.17 in the current study).

The upward shear stress on the shell surface ($\tau_{s/l}$) and shear stress at the mould side (τ_{mould}) are plotted in Figure 10. The variations in $\tau_{s/l}$ and τ_{mold} were inversely related to the variations in Q_{lub} and Q_t, respectively. The $\tau_{s/l}$ was within 29.62 to 209.75 Pa, τ_{mould} was within 18.55 to 19.54 kPa, and the maximum occurred when the mould was near the equilibrium position during the t_p. During the t_n, the $\tau_{s/l}$ decreased with the increase in slag consumption, reaching the minimum at the middle of t_n, and subsequently increased with a decrease in slag consumption. The τ_{mould} fluctuated around the minimum value of 18.55 kPa due to the fluctuation in lubrication slag consumption. The shear stress depended on the velocity gradient of the slag, slag viscosity, and the thickness of the solid and liquid slag films. Adequate slag consumption could reduce shear stress, avoid breakout, and be conductive to demould.

Conclusions

A two-dimensional coupled mathematical model was employed to study the infiltration and lubrication behaviour of the slag during continuous casting of steel. The infiltration velocity of slag and the pressure in the slag channel, the thickness of the liquid and solid slag layers, the total slag consumption, the lubrication slag consumption, and the shear stress of the liquid slag on the shell surface and at the mould wall were investigated. The conclusions can be summarized as follows.

- The mould oscillation led to periodic variations in the pressure and infiltration velocity in the slag channel. During the early and late stages of positive strip time (t_p), the slag flowed upward and the slag channel pressure was maximum negative pressure. At the middle of the negative strip time (t_n), infiltration velocity and the slag channel pressure reached maximum downward infiltration velocity and maximum positive pressure, respectively.
- The thickness variation of the solid slag layer was inversely related to that of the liquid slag layer, and was determined by the cooling strength and surface temperature of the shell. At the middle of the t_n, the thickness of the liquid layer with fast flowing slag became thinner and the solid layer became thicker.
- The variations of Q_{lub} and Q_t were similar. Slag consumption tended to increase during the t_n, and the peak values for Q_t

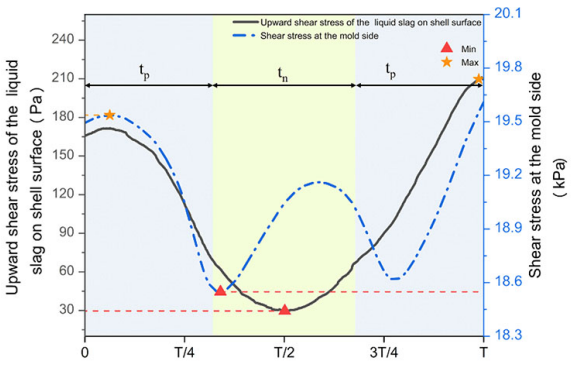

Figure 10—Upward shear stress of the liquid slag on the surface of the shell and shear stress at the moold side

and Q_{lub} were observed near the middle of t_n. The liquid slag was consumed from the middle and late period of t_p to the next early period of t_p, including the entire t_n.

➤ The $\tau_{s/l}$ and τ_{mould} were determined by $Q_{lu}b$ and Q_t, respectively, and gradually decreased with increasing slag consumption. The maximum $\tau_{s/l}$ and τ_{mould} occurred when the mould was near the equilibrium position during the t_p. The minimum $\tau_{s/l}$ and τ_{mould} occurred during the t_n.

Acknowledgements

This study was funded by Hebei Province Natural Science Fund (grant number E2020203128) and Hebei Education Department Higher Education Science and Technology Program (grant number ZD2021106).

Conflicts of Interest: The authors declare that they have no conflict of interest.

Data availability: The data that supports the findings of this study is available on request from the corresponding author.

References

Cao, M., Liu, Y., Yu, B., Zhou, C., and Zhang, X-Z. 2023. Modeling study on the initial solidification and formation of oscillation marks in continuous casting mold. *Transactions of the Indian Institute of Metals*, vol. 77. pp. 51–60. https://doi.org/10.1007/s12666-023-03040-x

Ji, J., Cui, Y., Zhang, X., Wang, Q., He, S., and Wang, Q. 2023. 3D coupled model on dynamic initial solidification and slag infiltration at the corner of slab continuous casting mold. *Steel Research International*, vol. 92. pp. 21–27. https://doi.org/https://doi.org/10.1002/srin.202100101

Jonayat, A.S.M. and Thomas, B.G. 2014. Transient thermo-fluid model of meniscus behavior and slag consumption in steel continuous casting. *Metallurgical and Materials Transactions B*, vol. 45. pp. 1842–1864. https://doi.org/10.1007/s11663-014-0097-9

Kölbl, N. and Harmuth, H. 2019. Automated break temperature determination of mould slags for the coninuous casting of steel based on temperature-dependent viscosity data. *Ironmaking & Steelmaking*, vol. 47. p. 899. https:doi.org/10.1080/03019233.2019.1639028

Louhenkilpi, S. 2014. Continuous casting of steel. *Treatise on Process Metallurgy*. Seetharaman, S. (ed.). Elsevier, Boston. Chapter 1.8.

Meng, Y. and Thomas, B.G. 2003. Modeling transient slag-layer phenomena in the shell/mold gap in continuous casting of steel. *Metallurgical and Materials Transactions B*, vol. 34. pp. 707–725. https://doi.org/10.1007/s11663-003-0041-x

Ramirez-Lopez, P., Lee, P., and Mills, K. 2010. Explicit modelling of slag infiltration and shell formation during mould oscillation in continuous casting. *ISIJ International*, vol. 50. pp. 425–434. https://doi.org/10.2355/isijinternational.50.425

Ramirez-Lopez, P., Lee, P., Mills, K., and Santillana, B. 2010. A new approach for modelling slag infiltration and solidification in a continuous casting mould. *ISIJ Intermational*, vol. 50. p. 1797. https://doi.org/10.2355/isijinternational.50.1797

Shin, H.J., Kim, S.H., Thomas, B.G., Lee, G-G., Park, J-M., and Sengupta, J. 2006. Measurement and prediction of lubrication, powder consumption, and oscillation mark profiles in ultra-low carbon steel slabs. *ISIJ International*, vol. 46. p. 1635. https://doi.org/10.2355/isijinternational.46.1635

Xiang, H.L., Xia, F., and Wu, G. 2023. Development and application of heat flux model of high casting speed billet mould. *Continuous Casting*, vol. 42. p, 21. https://www.chinamet.cn/Jweb_lz/EN/abstract/abstract154583.shtml

Yan, X., Jia, B., Wang, Q., He, S., and Wang, Q. 2019. Mold nonsinusoidal oscillation mode and its effect on slag infiltration for lubrication and initial shell growth during steel continuous casting. *Metals*, vol. 9. p. 418. https://doi.org/10.3390/met9040418

Yang, J., Chen, D., Long, M., and Guan, H. 2020. An approach for modelling slag infiltration and heat transfer in continuous casting mold for high Mn–high Al steel. *Metals*, vol. 10. p. 51. https://doi.org/10.3390/met10010051

Yang, J., Meng, X., and Zhu, M. 2014. Experimental study on mold flux lubrication for continuous casting. *Steel Research. Internstional*, vol. 85. p. 710. https://doi.org/10.1002/srin.201300232

Yang, J., Meng, X., and Zhu, M. 2018. Transient thermo-fluid and solidification behaviors in continuous casting mold: Oscillation behaviors. *ISIJ International*, vol. 58. p. 2071. https://doi.org/10.2355/isijinternational.ISIJINT-2018-169

Youming, W., Yeming, W., and Kuangdi, X. 2022. Continuous casting and continuous rolling. *ECPH Encyclopedia of Mining and Metallurgy*. Xu, K. (ed.). Springer Nature, Singapore.

Zhang, S., Wang, Q., He, S., and Wang, Q. 2018. Study of the mechanism of liquid slag infiltration for lubrication in slab continuous casting. *Metallurgical and Materials Transactions B*, vol. 49. pp. 2038–2049. https://doi.org/10.1007/s11663-018-1267-y

Zhang, X., Chen, W., Scheller, P.R., Ren, Y., and Zhang, L. 2019a. Mathematical modeling of initial solidification and slag infiltration at the meniscus of slab continuous casting mold. *JOM*, vol. 71. p. 78. https://doi.org/10.1007/s11837-018-3177-5

Zhang, X., Dan, Z., Chen, W., Zhang, L., and Wang, Q. 2021. Mathematical modeling on slag consumption and lubrication in a slab continuous casting mold. *Metallurgical and Materials Transactions B*, vol. 52. pp. 322–338. https://doi.org/10.1007/s11663-020-02022-4

Zhang, X., Chen, W., Ren, Y., and Zhang, L. 2019b. Mathematical modeling on the influence of casting parameters on initial solidification at t meniscus of slab continuous casting. *Metallurgical and Materials Transactions B*. vol. 50. pp. 1444–1460. https://doi.org/10.1007/s11663-019-01570-8 ◆